IBS Center for Climate Physics

EGU General Assembly 2020

ICCP

Ultra-high-resolution future coupled model projections of atmospheric rivers

Arjun Babu Nellikkattil[1,2], Bin Guan[3,4], June-Yi Lee[1,2,5], Axel Timmermann[1,2], Sun-Seon Lee[1], Duane Waliser[4], Jung-Eun Chu[1]

Center for Climate Physics, Institute for Basic Science, Busan, South Korea[1]
Department of Climate System, Pusan National University, Busan, South Korea[2]
Joint Institute for Regional Earth System Science and Engineering, University of California, Los Angeles[3]
Jet Propulsion Laboratory, California Institute of Technology[4]
Research Center for Climate Sciences, Pusan National University, Busan, South Korea[5]

Introduction & Motivation

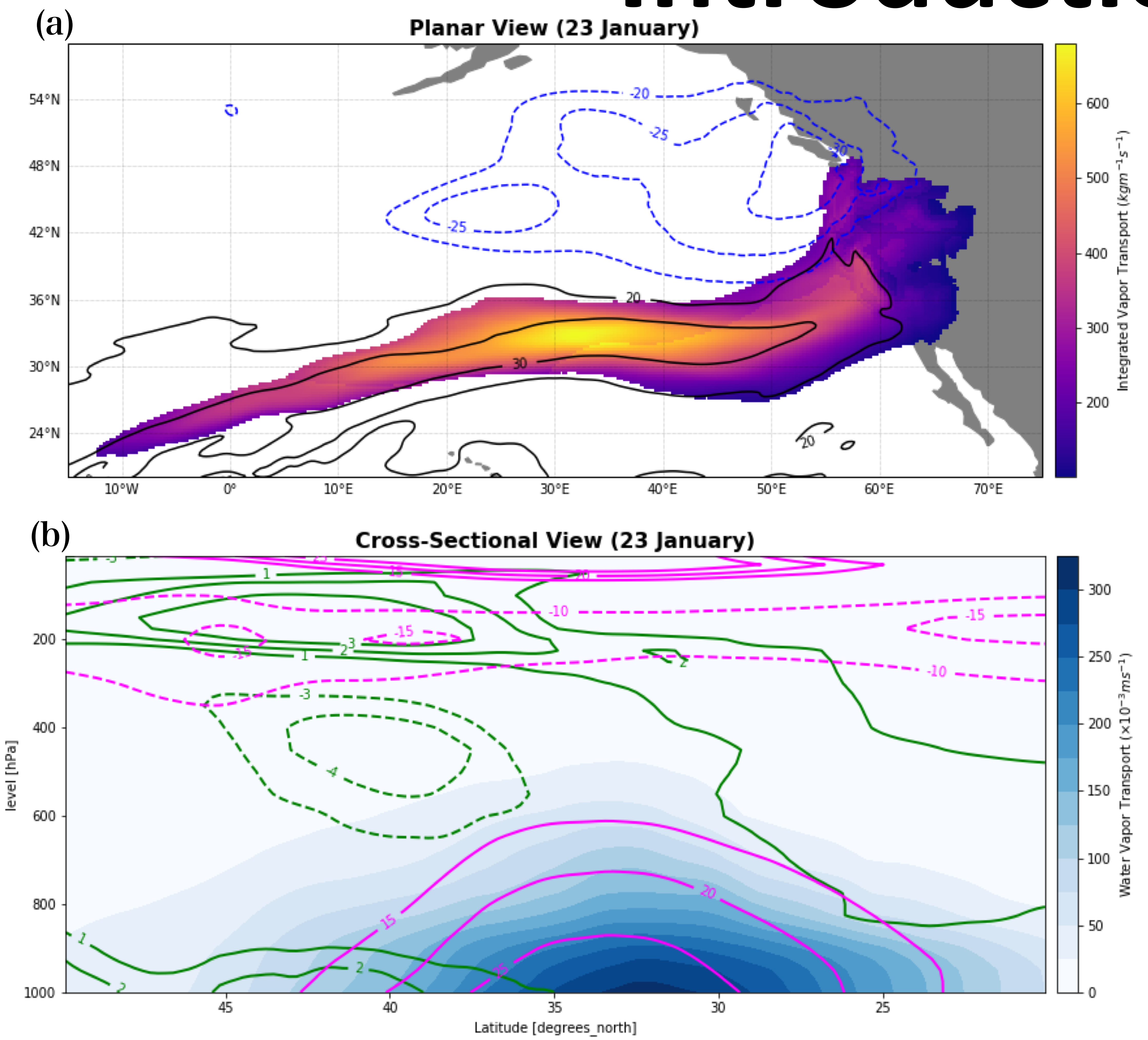

Figure 1: An example of a detected AR in CESM1.2.2 high-resolution simulation for present day conditions. (a) shows the detected shape with filled contours indicating the integrated water vapor transport. The black contours represents the total precipitable water in kg/m^2 while the blue contours shows the surface pressure anomaly. (b) is the latitudinal cross section of AR in (a). The filled contours represent the water vapor transport. The magenta and green contours are the anomalous horizontal wind(ms^{-1}) and air temperature(K) respectively.

1. Atmospheric Rivers (ARs) are defined as a long narrow region of strong horizontal water vapor transport[1].
2. At any instant of time ARs transport significant quantity of total water vapor transport across midlatitudes[2].
3. ARs play a significant role in the total annual and well as extreme precipitation along the coastal regions where they make landfalls[3].
4. Although ARs are manifested as a large-scale synoptic weather phenomenon, they interact significantly with the topography which is better resolved in a ultra-high resolution simulation.
5. A high-resolution modeling framework is also expected to provide more realistic precipitation patterns[4].

Data and Methods

To detect ARs, we followed [5]. As evident from the definition ARs should have high Integrated Vapor Transport (IVT) and should satisfy a certain geometric criterion with considerable amount of coherent poleward transport. Where IVT is defined as,

$$IVT = \sqrt{(IVT_x + IVT_y)^2} \quad \text{and,} \quad IVT_x = \frac{-1}{g}\int_{1000hpa}^{300hpa} Uq\,dp, \quad IVT_y = \frac{-1}{g}\int_{1000hpa}^{300hpa} Vq\,dp$$

a. The IVT threshold: A point is identified as part of an AR if the IVT is greater than the 85th percentile of daily IVT values taken over a period of 5 months centered on the current month over all the years at the grid point, or 100 $kgm^{-1}s^{-1}$, whichever is larger.

b. The directional requirement: Structures that have pixels that deviate by more than 45^0 from the mean direction in more than half of the area of the structure is also removed from the analysis. Those structures without a significant poleward transport (50 $kgm^{-1}s^{-1}$) are also removed.

c. The geometry requirement: Once the objects satisfying (a) and (b) is identified, only those with length longer than 2000 km and a length to width ratio higher than 2 is identified as ARs.

d. Landfall: ARs identified in the previous three steps are examined to see if they cross a grid point with land fraction > 0.5 and with IVT directed onshore. If so, these will be identified as landfalling ARs.

Datasets Used:

To detect ARs we used daily mean Horizontal Velocity (U,V) and Specific humidity (q) and land-sea mask from the following datasets

1. Fully coupled CESM1.2.2 High Resolution Simulation: The atmospheric component was simulated with a horizontal resolution of around 0.25° and 30 vertical layers. We conducted three experiments with different level of fixed greenhouse gas condition: (1) present day (PD) (CO_2 concentration of 367 ppm), (2) doubling CO_2 (2xCO2)(734 ppm), and (3) quadrupling CO_2(4xCO2) (1468 ppm). AR detection algorithm is run on the 20 year period after letting the model run for 70, 80 and 80 years respectively.

Validation

Source: Guan and Waliser (2015)

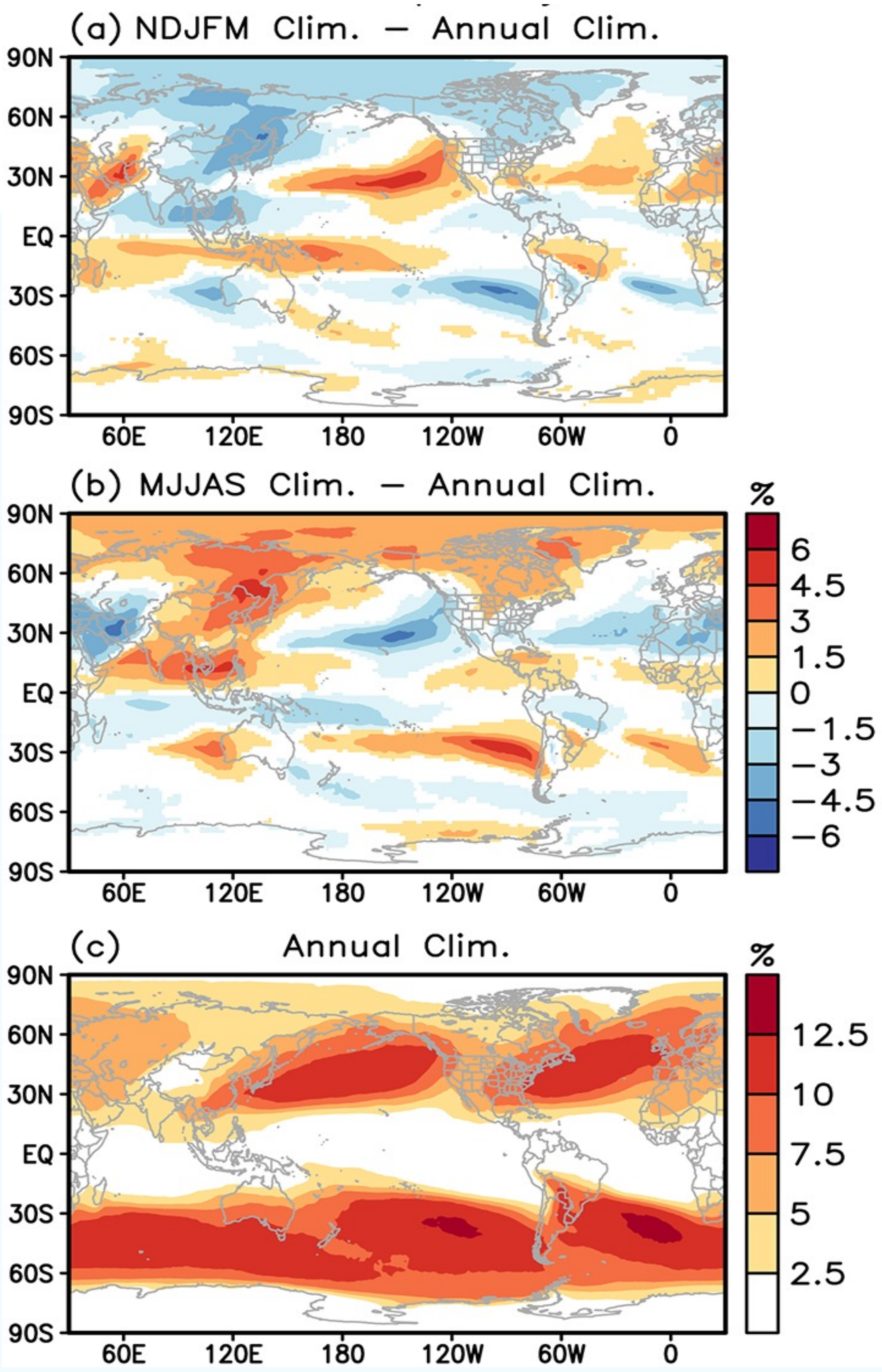

ERA-Interim (1997-2014)

Figure 3: (a–c) AR frequency (percent of time steps) in (Figure 3a) NDJFM (November-March) and (Figure 3b) MJJAS (May to September with (Figure 3c) the annual AR frequency subtracted. In Figures 3a, 3b values are shown only if they are statistically significant at the 95% level. The calculation were made using ERA-Interim data 6 hourly data for the period of 1997–2014

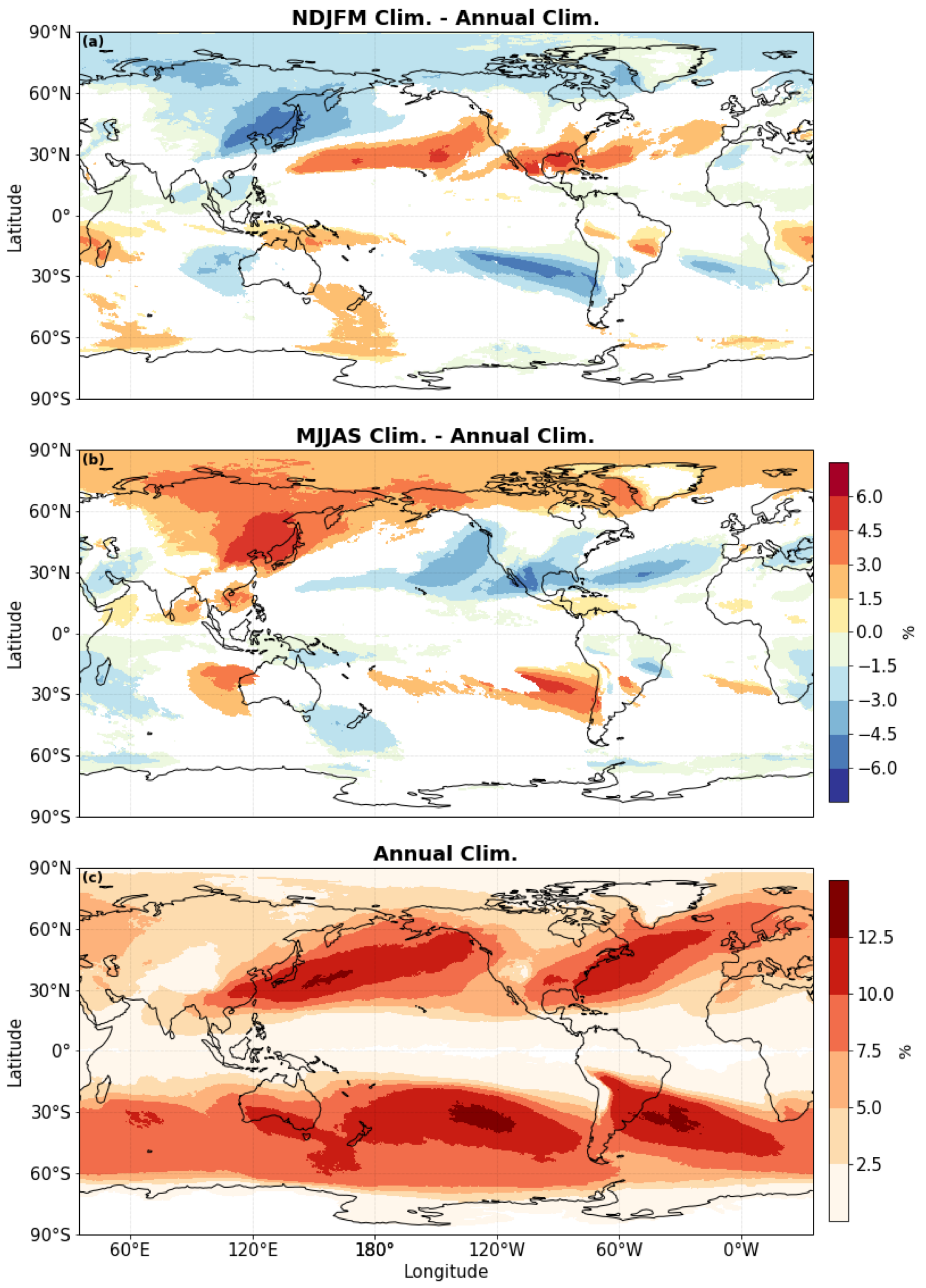

CESM1.2.2 PD (20 Years)

Figure 4: Same as shown in figure 3 but for daily mean CESM ultra high resolution for present day(PD) simulation.

- CESM1.2.2 high resolution run can simulate realistic AR frequency reasonably well.
- The southern Indian ocean has fewer AR days compared to the observations

Response to GHG Forcing

Figure 5: Changes in mean AR frequency with respect to the PD run. Values are shown only if they are statistically significant at the 95% level in a two tailed t-test

1. The overall changes quantitatively agree with the previous studies (e.g. [6]) except for the statistically significant reduction seen in the southern midlatitudes
2. Maximum enhancement of AR activity is seen along the elevated topographic regions and southern ocean.

Summary

Characteristics	2xCO2 Present Day Threshold	4xCO2 Present Day Threshold	Espinoza et.al. 2018 (RCP 8.5)
Mean Global Frequency	Increase ~42%	Increase ~61%	Increase by ~49%
Total Counts	Decrease by ~6%	Decrease by ~30%	Decrease by ~10 %
Mean Length	Increase by ~20%	Increase by ~42%	Increase by ~25%
Mean Width	Increase by ~18%	Increase by ~42%	Increase by ~25%
Total Landfalling counts	Increase by ~13.5%	Increase by 4%	-
Mean IVT Transport	Increase by ~2.5%	Increase by ~4.4%	Increase by 25%

Table 1: Changes seen in AR characteristics in response to GHG warming is summarized. A recently published study[6] is also included for reference

Conclusions and Caveats

1. In this preliminary study, we show the response of ARs to increased greenhouse gas forcing using AR detection methods developed by Guan and Waliser (2015).
2. In concurrence with recent studies, the global AR frequency is enhanced in response to warming. The enhancement is most pronounced along the topographic barriers and southern ocean. The topography-AR activity interaction needs further investigation.
3. Using IVT thresholds from PD run, would lead to "fattening" of ARs in 2xCO2 and 4xCO2 runs resulting in non-detection of some regions with strong IVT. This would be fixed in a later version.
4. The impact of these changes in winds and precipitation extreme events will be discussed in future.
5. A lack of comprehensive theory governing the formation, maintenance and decay of ARs makes it harder to understand the response of ARs. Some uncertainty is also introduced by the choice of detection methods. Lagrangian Coherent Structure (LCS) analysis is being implemented to study these in detail.

References

1) Ralph, F. M., Dettinger, M. D., Cairns, M. M., Galarneau, T. J., & Eylander, J. (2018). Defining "atmospheric river": How the Glossary of Meteorology helped resolve a debate. Bulletin of the American Meteorological Society, 99(4), 837-839.
2) Zhu, Y., & Newell, R. E. (1998). A proposed algorithm for moisture fluxes from atmospheric rivers. Monthly weather review, 126(3), 725-735.
3) Ralph, F. M., & Dettinger, M. D. (2011). Storms, floods, and the science of atmospheric rivers. Eos, Transactions American Geophysical Union, 92(32), 265-266.
4) Small, R. J., Bacmeister, J., Bailey, D., Baker, A., Bishop, S., Bryan, F., ... & Jochum, M. (2014). A new synoptic scale resolving global climate simulation using the Community Earth System Model. Journal of Advances in Modeling Earth Systems, 6(4), 1065-1094.
5) Guan, B., & Waliser, D. E. (2015). Detection of atmospheric rivers: Evaluation and application of an algorithm for global studies. Journal of Geophysical Research: Atmospheres, 120(24), 12514-12535.
6) Espinoza, V., Waliser, D. E., Guan, B., Lavers, D. A., & Ralph, F. M. (2018). Global analysis of climate change projection effects on atmospheric rivers. Geophysical Research Letters, 45(9), 4299-4308.